Leakage Minimization in Network-Assisted Full-Duplex Cell-Free Massive MIMO Systems

Koushi Okui*, Kengo Ando†, Giuseppe Abreu ‡ and Koji Ishibashi§,
*§Advanced Wireless & Communication Research Center (AWCC), The University of Electro-Communications,
1–5–1 Chofugaoka, Chofu, Tokyo 182-8585, Japan
† ‡ School of Computer Science and Engineering, Constructor University Campus Ring 1, 28759, Bremen, Germany
Emails: *okui@awcc.uec.ac.jp, †kando@constructor.university, ‡gabreu@constructor.university §koji@ieee.org

***Abstract*—We propose a new scheme for the joint design of access point clustering and leakage-minimization beamforming in a network-assisted full-duplex (NAFD) cell-free massive multiple-input multiple-output (CF-mMIMO) system. In the proposed method, each user considers all other users as eavesdroppers or malicious users, with the corresponding secrecy capacity formulated as the difference between the channel capacity of the intended user and the maximum leakage to the other users. By maximizing this secrecy capacity, the proposed minimizes information leakage to other users while maintaining high spectral efficiency for each user. As a result, the proposed approach achieves approximately double spectral efficiency and confidentiality compared to conventional CF-mMIMO based on time division duplex.**

***Index Terms*—Cell-free massive MIMO, network-assisted full-duplex, convex optimization.**

I. Introduction

With the widely spreading of information technologies and the expansion of their applications, wireless communication systems need to satisfy the requirements not only for a higher data rate but also for highly secure communications. Notably, wireless communication systems always face the possibility of information leakage to the inherently public nature of wireless transmissions. To further complicate the scenario, the number of applications dealing with private and critical data is increasing, and the research on quantum computers, which are capable to break classical encryption-based security schemes, is progressing fast.

In order to increase the security of wireless systems, countermeasures against eavesdropping by malicious users are essential, which makes the use of physical-layer (also known as information-theoretic) security attractive, as it can which can enhance classical security techniques in a complementary fashion [1], [2]. Information-theoretic/physical-layer security is based on the notion of secrecy capacity, defined as the difference between the communication channel capacities of the legitimate receiver and the eavesdropper, which represents the maximum communication capacity of confidential communication achievable by the legitimate receiver when the amount of information leakage to the eavesdropper is set to zero [3].

In order to guarantee information-theoretic security to each user equipment (UE) and to prevent eavesdropping by malicious UEs in the network, it is essential that the channel capacity among UEs is equitable. In typical cellular networks, it is known that the channel capacity of a UEs at the edge of a cell is lower than those of UEs closer to the base station [4]–[6]. In such cases, it is difficult to prevent eavesdropping by malicious UEs close to the base station.

One of the solutions to ensure fair communication quality for all UEs in a network is, therefore, the cell-free massive multiple-input multiple-output (CF-mMIMO) network architecture [4]–[7]. In CF-mMIMO systems, distributed access points (APs), which transmit and receive signals to and from the UEs, are connected to a central processing unit (CPU) via a fronthaul for a collaborative signal processing. Taking advantage of both the distributed nature and high number of spatial degrees-of-freedom (DoF) of the architecture, CF-mMIMO systems can be optimized to enhance the secrecy if the links to its users. As an example, in [7], the authors reformulate the secrecy capacity as the difference in the channel capacity between the intended communication information and the maximum information leakage to other UEs, regarding all other UEs as potential eavesdroppers for each UE. A beamforming design was than proposed which can maximize the secrecy performance in terms of secrecy capacity while preserving high spectral efficiency (SE) for the entire CF-mMIMO system.

The latter work assumes, however time division duplex (TDD) access, while it known that the SE of TDD-based CF-mMIMO systems degrades when communication requests, whether for uplink or for downlink, are unevenly distributed over the network [8], [9]. A solution to the latter problem is network-assisted full-duplex (NAFD) CF-mMIMO [8], [9], where full-duplex communication over a given service area is realized by assigning each AP to either uplink or downlink transmission. It has been shown that and NAFD-CF-mMIMO can achieve higher SE than the TDD-based CF-mMIMO, thanks to sophisticated AP allocation and beamforming design which are capable of mitigating the mutual interference between uplink and downlink transmissions [10]–[12].

In light of the above, we propose a beamforming design and AP clusterization to maximize the secrecy capacity of NAFD-CF-mMIMO systems, aiming at combining the advantages of the leakage-minimization approach of [7] and the fairness-enhancing and rate-maximization approaching performance of [8], [9] via the maximization of the geometric mean of the system's secrecy capacity.

Numerical results confirm that the NAFD-CF-mMIMO with the proposed beamforming and AP clustering can achieve better performance than TDD in terms of both secrecy capacity and communication SE.

The following notation is used throughout the article. The symbols $\mathbf{v}$ and $\mathbf{V}$ denote column vectors and matrices. The complex conjugate transpose and the vector diagonalization are denoted by $(\cdot)^{\mathrm{H}}$, and $\mathrm{diag}(\cdot)$, respectively. The complex Gaussian distribution with mean a and variance b is denoted by $\mathcal{CN}(a, b)$. The l_2 norm is denoted by $\|\cdot\|$.

II. System Model

Consider a NAFD-CF-mMIMO system composed of K single-antenna UEs, one CPU, and M spatially distributed single-antenna APs, which are interconnected to the common CPU via fronthaul link. For the sake of latter convenience, the sets of UEs and APs are defined as $\mathcal{K} \triangleq \{1, ..., K\}$ and $\mathcal{M} \triangleq \{1, ..., M\}$, respectively.

Assuming that each UE requests only one-way communication, whether uplink or downlink, the sets of UEs requesting uplink and downlink can be respectively represented as $\mathcal{K}_{\mathrm{ul}} \triangleq \{1, ..., k_{\mathrm{ul}}, ..., K_{\mathrm{ul}}\} \subset \mathcal{K}$, $\mathcal{K}_{\mathrm{dl}} \triangleq \{1, ..., k_{\mathrm{dl}}, ..., K_{\mathrm{dl}}\} \subset \mathcal{K}$ with $K = K_{\mathrm{ul}} + K_{\mathrm{dl}}$ and $\mathcal{K}_{\mathrm{ul}} \cap \mathcal{K}_{\mathrm{dl}} = \emptyset$. The channel vector between the APs and the k-th UE is defined as $\mathbf{h}_k \triangleq [h_{1,k}, ..., h_{M,k}]^{\mathrm{T}} \in \mathbb{C}^{M\times 1}$, and the channel matrix among all the APs is also defined as $\mathbf{H} \in \mathbb{C}^{M\times M}$. Each channel coefficient is characterized by large-scale fading $\beta \in \mathbb{R}^+$ corresponding to the path loss and shadowing [13] and small scale fading $g \sim \mathcal{CN}(0, 1)$ so that the (i, j)-th element of a channel vector or matrix can be defined as $h_{i,j} \triangleq \sqrt{\beta_{i,j}} g_{i,j}$.

A. Data Transmission

In NAFD systems, although each AP itself does not operate in full duplex, system-wise full duplex communication is realized by well-designed assignment of each AP to either uplink or downlink. For the sake of latter convenience, the assignment of the m-th AP for communicating the k-th UE is represented by the variable $d_{mk} \in \{0, 1\}$ (*i.e.*, assigned $d_{m,k} = 1$ or unassigned $d_{m,k} = 0$), and matrix $\mathbf{D}_k \triangleq \mathrm{diag}(d_{1,k}, ..., d_{M,k}) \in \{0, 1\}^{M\times M}$. The signal vector of downlink symbols transmitted from all the APs is given by

$$\mathbf{x} = \sum_{k\in\mathcal{K}_{\mathrm{dl}}} \mathbf{D}_k \mathbf{w}_k s_k^{\mathrm{dl}} \in \mathbb{C}^{M\times 1}, \tag{1}$$

where $\mathbf{w}_k \triangleq [w_{1,k}, ..., w_{M,k}]^{\mathrm{T}} \in \mathbb{C}^{M\times 1}$ represents the precoding vector designed by the CPU, and $P_{\max} \in \mathbb{R}^+$ denotes the maximum transmit power for each AP, satisfying $\sum_{k\in\mathcal{K}_{\mathrm{dl}}} |w_{m,k}|^2 \le P_{\max}$.

In the above, $s_k^{\mathrm{dl}} \sim \mathcal{CN}(0, 1)$ is the downlink data signal for the k-th UE, whose estimate is given by

$$\hat{s}_k^{\mathrm{dl}} = \sum_{k'\in\mathcal{K}_{\mathrm{dl}}} \mathbf{h}_k^{\mathrm{H}} \mathbf{D}_{k'} \mathbf{w}_{k'} s_{k'}^{\mathrm{dl}} + \sum_{k'\in\mathcal{K}_{\mathrm{ul}}} \sqrt{p_{k'}^{\mathrm{ul}}} h_{k,k'} s_{k'}^{\mathrm{ul}} + n_k, \tag{2}$$

where $p_k^{\mathrm{ul}} \in \mathbb{R}^+$ represents the uplink UE's transmit power, $n_k \sim \mathcal{CN}(0, \sigma_{\mathrm{dl}}^2)$ denotes the additive white Gaussian noise (AWGN) at the k-th UE, $h_{k,k'}$ represents the channel between UEs, and $s_{k'}^{\mathrm{ul}} \sim \mathcal{CN}(0, 1)$ is the data signal from the k'-th uplink UE.

For uplink data transmission, the received signal vector $\mathbf{r} \in \mathbb{C}^{M\times 1}$ is given by

$$\mathbf{r} = \sum_{k\in\mathcal{K}_{\mathrm{ul}}} \sqrt{p_k^{\mathrm{ul}}} \mathbf{h}_k s_k^{\mathrm{ul}} + \mathbf{H}^{\mathrm{H}} \mathbf{x} + \mathbf{n} \in \mathbb{C}^{M\times 1}, \tag{3}$$

where $\mathbf{n} \sim \mathcal{CN}(0, \sigma_{\mathrm{ul}}^2 \mathbf{I}_M)$ denotes the AWGN at all APs, and such that when the combiner $\mathbf{v}_k \in \mathbb{C}^{M\times 1}$ is applied at the AP side to the received signal, the corresponding estimated signal for the k-th UE can be expressed as

$$\hat{s}_k^{\mathrm{ul}} = \sum_{k'\in\mathcal{K}_{\mathrm{ul}}} \sqrt{p_{k'}^{\mathrm{ul}}} \mathbf{v}_k^{\mathrm{H}} \mathbf{D}_k \mathbf{h}_{k'} s_{k'}^{\mathrm{ul}} + \mathbf{v}_k^{\mathrm{H}} \mathbf{D}_k \mathbf{H}^{\mathrm{H}} \mathbf{x} + \mathbf{v}_k^{\mathrm{H}} \mathbf{D}_k \mathbf{n}. \tag{4}$$

From equations (2) and (4), the signal-to-interference plus noise ratios (SINRs) for the k-th UE in uplink and downlink transmission are respectively defined as

$$\eta_k^{\mathrm{I}} \triangleq \begin{cases} \dfrac{p_k^{\mathrm{ul}} |\mathbf{v}_k^{\mathrm{H}} \mathbf{D}_k \mathbf{h}_k|^2}{\mathrm{IPN}_k^{\mathrm{I}}} & k \in \mathcal{K}_{\mathrm{ul}}, \\ \dfrac{|\mathbf{h}_k^{\mathrm{H}} \mathbf{D}_k \mathbf{w}_k|^2}{\mathrm{IPN}_k^{\mathrm{I}}} & k \in \mathcal{K}_{\mathrm{dl}}, \end{cases} \tag{5}$$

where the denominator $\mathrm{IPN}_k^{\mathrm{I}}$ in equation (5) is defined by equation (6) shown at the top of the next page.

Then, the SE for the k-th UE is finally given by

$$\zeta_k^{\mathrm{I}} \triangleq \mathbb{E}\left[\log_2(1 + \eta_k^{\mathrm{I}})\right], \ \forall k \in \mathcal{K}. \tag{7}$$

B. Information Leakage Model

This paper considers secrecy-oriented NAFD-CF-mMIMO systems that mitigate information leakage to keep the privacy of each UE by regarding all downlink UEs in the system as potentially eavesdroppers. For the sake of readability, the UE index of the potential eavesdropper in the downlink UE is defined by $e \in \mathcal{K}_{\mathrm{dl}}$. It is further assumed that the $e \in \mathcal{K}_{\mathrm{dl}}$-th UE tries to eavesdrop on the signal for k-th uplink or downlink UE by demodulation and removal of its own data from the received signal via ideal successive interference cancellation [7]. Then, the estimate of the k-th UE's signal at $e \in \mathcal{K}_{\mathrm{dl}}$-th UE can be given as

$$\hat{s}_{e,k} = \sum_{k'\in\mathcal{K}_{\mathrm{dl}\setminus\{e\}}} \mathbf{h}_e^{\mathrm{H}} \mathbf{D}_{k'} \mathbf{w}_{k'} s_{k'}^{\mathrm{dl}} + \sum_{k'\in\mathcal{K}_{\mathrm{ul}}} \sqrt{p_{k'}^{\mathrm{ul}}} h_{e,k'} s_{k'}^{\mathrm{ul}} + n_k. \tag{8}$$

From (8), the SINR of eavesdropping by the e-th UE on the k-th uplink or downlink UE can be expressed as

$$\eta_{e,k}^{\mathrm{L}} \triangleq \begin{cases} \dfrac{p_k^{\mathrm{ul}} |h_{e,k}|^2}{\mathrm{IPN}_{e,k}^{\mathrm{L}}} & k \in \mathcal{K}_{\mathrm{ul}}, \\ \dfrac{|\mathbf{h}_e^{\mathrm{H}} \mathbf{D}_k \mathbf{w}_k|^2}{\mathrm{IPN}_{e,k}^{\mathrm{L}}} & k \in \mathcal{K}_{\mathrm{dl}}, \end{cases} \tag{9}$$

where $\mathrm{IPN}_{e,k}^{\mathrm{L}}$ in the denominator of the above equation is given by (10) shown at the top of this page.

From the above, it follows that the achievable SE for potential eavesdroppers can be given by

$$\zeta_{e,k}^{\mathrm{L}} \triangleq \mathbb{E}\left[\log_2(1 + \eta_{e,k}^{\mathrm{L}})\right]. \tag{11}$$

$$\mathrm{IPN}_k^{\mathrm{I}} \triangleq \begin{cases} \sum\limits_{k' \in \mathcal{K}_{\mathrm{ul}} \backslash \{k\}} p_{k'}^{\mathrm{ul}} |\mathbf{v}_k^{\mathrm{H}} \mathbf{D}_k \mathbf{h}_{k'}|^2 + \sum\limits_{k' \in \mathcal{K}_{\mathrm{dl}}} |\mathbf{v}_k^{\mathrm{H}} \mathbf{D}_k \mathbf{H}^{\mathrm{H}} \mathbf{D}_{k'} \mathbf{w}_{k'}|^2 + \sigma_{\mathrm{ul}}^2 \|\mathbf{v}_k^{\mathrm{H}} \mathbf{D}_k\|^2, & k \in \mathcal{K}_{\mathrm{ul}} \\ \sum\limits_{k' \in \mathcal{K}_{\mathrm{dl}} \backslash \{k\}} |\mathbf{h}_k^{\mathrm{H}} \mathbf{D}_{k'} \mathbf{w}_{k'}|^2 + \sum\limits_{k' \in \mathcal{K}_{\mathrm{ul}}} p_{k'}^{\mathrm{ul}} |h_{k,k'}|^2 + \sigma_{\mathrm{dl}}^2, & k \in \mathcal{K}_{\mathrm{dl}} \end{cases} \tag{6}$$

$$\mathrm{IPN}_{e,k}^{\mathrm{L}} \triangleq \begin{cases} \sum\limits_{k' \in \mathcal{K}_{\mathrm{ul}} \backslash \{k,e\}} p_{k'}^{\mathrm{ul}} |h_{e,k'}|^2 + \sum\limits_{k' \in \mathcal{K}_{\mathrm{dl}}} |\mathbf{h}_e \mathbf{w}_{k'}|^2 + \sigma_{\mathrm{dl}}^2, & k \in \mathcal{K}_{\mathrm{ul}} \\ \sum\limits_{k' \in \mathcal{K}_{\mathrm{dl}} \backslash \{k,e\}} |\mathbf{h}_e^{\mathrm{H}} \mathbf{D}_{k'} \mathbf{w}_{k'}|^2 + \sum\limits_{k' \in \mathcal{K}_{\mathrm{ul}}} p_{k'}^{\mathrm{ul}} |h_{e,k'}|^2 + \sigma_{\mathrm{dl}}^2, & k \in \mathcal{K}_{\mathrm{dl}} \end{cases} \tag{10}$$

Assuming each $e \in \mathcal{K}_{\mathrm{dl}} \backslash \{k\}$-th UE acts independently, the worst-case information leakage is defined as

$$\zeta_{e_k}^{\tilde{\mathrm{L}}} \triangleq \max_{k \neq e} \zeta_{e,k}^{\mathrm{L}} \quad \text{with} \quad \eta_{e_k}^{\tilde{\mathrm{L}}} \triangleq \max_{k \neq e} \eta_{e,k}^{\mathrm{L}}. \tag{12}$$

From the above, we define the secrecy capacity by the achievable SE of k-th UE subjected to the information leakage to the $e \in \mathcal{K}_{\mathrm{dl}} \backslash \{k\}$-th UE.

$$\psi_k \triangleq \max \left[\zeta_k^{\mathrm{I}} - \zeta_{e_k}^{\tilde{\mathrm{L}}},\ 0 \right], \forall k \in \mathcal{K}. \tag{13}$$

III. Joint Design of Beamforming & AP Clustering

In this section, we propose a joint design of AP clustering and beamforming that maximizes the secrecy capacity defined in the above. In general, the sum rate maximization follows the water-filling theorem, such that more transmit power can be allocated to the UEs with better channel state information (CSI). As a result of the aforementioned sum rate maximization approach, however, UEs with worse CSIs may not be allocated enough power for communication, which may result in outage. Therefore, in order to increase the likelihood that information-theoretic security is offered to all UEs, it is essential to maximize not only the aggregate secrecy capacity, but also the secrecy capacity of each individual UE. Furthermore, it is known that when a NAFD-CF-mMIMO system is optimized to maximize the sum SE, the achievable SEs of the uplink are typically significantly lower than that of downlink, due to the asymmetry of transmit power between uplink and downlink communications. In order to avoid these problems, geometric mean maximization of SEs is considered so as to realize user fairness in conjunction with SE maximization [8].

In light of the above, this paper proposes a simultaneous AP clustering and beamforming design to maximize the geometric mean of the secrecy capacity for each UE, which can be formulated as

$$\underset{\mathbf{w}_k, \mathbf{v}_k, \mathbf{D}_k}{\text{maximize}} \quad \left(\prod_{k \in \mathcal{K}} \psi_k \right)^{\frac{1}{K}} \tag{14a}$$

$$\text{subject to} \quad d_{mk} \in \{0,1\}, \forall m \in \mathcal{M}, \forall\ k \in \mathcal{K}, \tag{14b}$$

$$d_{mk_{\mathrm{ul}}} + d_{mk_{\mathrm{dl}}} \leq 1, \forall m \in \mathcal{M}, \forall k \in \mathcal{K}, \tag{14c}$$

$$1 \leq \textstyle\sum_{m \in \mathcal{M}} d_{mk}, \forall k \in \mathcal{K}, \tag{14d}$$

$$\textstyle\sum_{m \in \mathcal{M}} d_{mk} \leq T, \forall k \in \mathcal{K}, \tag{14e}$$

$$\textstyle\sum_{k \in \mathcal{K}_{\mathrm{dl}}} |w_{mk} d_{mk}|^2 \leq P_{\max}, \forall m \in \mathcal{M}, \tag{14f}$$

$$\textstyle\sum_{k \in \mathcal{K}_{\mathrm{ul}}} |v_{mk} d_{mk}|^2 \leq 1, \forall\ m \in \mathcal{M}, \tag{14g}$$

where T is a constant that represents the maximum number of APs that can be assigned to each UE, and equations (14f) and (14g) are power constraints for the precoder and combiner, respectively.

Since the function ψ_k in the objective of equation (14) is not convex, the problem cannot be solved efficiently. In order to convexize ψ_k, the lagranian dual transform (LDT) and quadratic transform (QT) can be applied to relax it to a convex function [14]–[16], which yields

$$f^{\mathrm{o}}(\mathbf{w}_k, \mathbf{v}_k, \mathbf{D}_k) = \left(\prod_{k \in \mathcal{K}} \zeta_k^{\mathrm{conv,I}} \right)^{\frac{1}{K}} + \sum_{k \in \mathcal{K}} \zeta_{e_k}^{\mathrm{conv,L}}, \tag{15}$$

where $\zeta_k^{\mathrm{conv,I}}$ is defined by

$$\zeta_k^{\mathrm{conv,I}} \triangleq \Omega_k^{\mathrm{I}} + \Upsilon_k^{\mathrm{I}} \Re\{s_k^{\mathrm{I}} \Gamma_k^{\mathrm{I},1}\} - |s_k^{\mathrm{I}}|^2 \Gamma_k^{\mathrm{I},2},\ \forall k \in \mathcal{K} \tag{16}$$

while the remaining quantities are defined as $\Omega_k^{\mathrm{I}} \triangleq \log_2(1+\eta_k^{\mathrm{I}}) - \eta_k^{\mathrm{I}}$, $\Upsilon_k^{\mathrm{I}} \triangleq 2\sqrt{1+\eta_k^{\mathrm{I}}}$, and $s_k^{\mathrm{I}} \triangleq \Gamma_k^{\mathrm{I},1} \sqrt{1+\eta_k^{\mathrm{I}}} / \Gamma_k^{\mathrm{I},2}$.

In the above, the quantity $\Gamma_k^{\mathrm{I},1}$ is expressed by the following equation and $\Gamma_k^{\mathrm{I},2}$ is shown at the top of the next page.

$$\Gamma_k^{\mathrm{I},1} \triangleq \begin{cases} \sqrt{p_k^{\mathrm{ul}}} \mathbf{v}^{\mathrm{H}} \mathbf{h}_k & k \in \mathcal{K}_{\mathrm{ul}}, \\ \mathbf{h}^{\mathrm{H}} \mathbf{w}_k & k \in \mathcal{K}_{\mathrm{dl}}. \end{cases} \tag{17}$$

Similarly to $\zeta_{e_k}^{\mathrm{conv,I}}$, the quantity $\zeta_{e_k}^{\mathrm{conv,L}}$ is also given by

$$\zeta_{e_k}^{\mathrm{conv,L}} \triangleq \Omega_{e_k}^{\mathrm{L}} + \Upsilon_{e_k}^{\mathrm{L}} \Re\{s_{e_k}^{\mathrm{L}} \Gamma_{e_k}^{\mathrm{L},1}\} - |s_{e_k}^{\mathrm{L}}|^2 \Gamma_{e_k}^{\mathrm{L},2},\ \forall k \in \mathcal{K}, \tag{19}$$

with the remaining quantities in equation (19) respectively given by $\Omega_{e_k}^{\mathrm{L}} \triangleq \log_2(1+\tilde{\eta}_{e_k}^{\mathrm{L}})^{-1} - \eta^{\tilde{\mathrm{L}}}{}_{e_k}^{-1}$, $\Upsilon_{e_k}^{\mathrm{L}} \triangleq 2\sqrt{(1+\tilde{\eta}_{e_k}^{\mathrm{L}})^{-1}}$, and $s_{e_k}^{\mathrm{L}} \triangleq \Gamma_{e_k}^{\mathrm{L},1} \sqrt{(1+\tilde{\eta}_{e_k}^{\mathrm{L}})^{-1}} / \Gamma_{e_k}^{\mathrm{L},2}$.

In the above, $\Gamma_{e_k}^{\mathrm{L},1}$ is given in equation (21) at the top of the next page, while $\Gamma_{e_k}^{\mathrm{L},2}$ is given by

$$\Gamma_{e_k}^{\mathrm{L},2} \triangleq \begin{cases} \sqrt{p_k^{\mathrm{ul}}} h_{e_k,k} & k \in \mathcal{K}_{\mathrm{ul}}, \\ \mathbf{h}_{e_k}^{\mathrm{H}} \mathbf{w}_k & k \in \mathcal{K}_{\mathrm{dl}}. \end{cases} \tag{20}$$

Although the objective of problem (14) is relaxed into a convex function via the LDT and QT, as shown above, the problem itself is still not convex due to the discrete-valued constraint on $d_{mk} \in \{0,1\}$, which makes the problem a mixed integer programming problem. And while the continuous relaxation of the discrete constraints into $d_{mk} \in [0,1]$ could be used to convexize the entire problem, this approach causes misalignment by approximating the discrete values into continuous.

$$\Gamma_k^{\mathrm{I},2} \triangleq \begin{cases} \sum\limits_{k' \in \mathcal{K}_{\mathrm{ul}} \setminus \{k\}} p_{k'}^{\mathrm{ul}} \mathbf{v}_k^{\mathrm{H}} \mathbf{h}_{k'} \mathbf{h}_{k'}^{\mathrm{H}} \mathbf{v}_k + \mathbf{v}_k^{\mathrm{H}} \mathbf{H}^{\mathrm{H}} (\tilde{\mathbf{x}})^{t-1} (\tilde{\mathbf{x}}^{\mathrm{H}})^{t-1} \mathbf{H} \mathbf{v}_k + \sigma_{\mathrm{ul}}^2 \|\mathbf{v}_k^{\mathrm{H}}\|^2, k \in \mathcal{K}_{\mathrm{ul}} \\ \sum\limits_{k' \in \mathcal{K}_{\mathrm{dl}} \setminus \{k\}} \mathbf{h}_k^{\mathrm{H}} \mathbf{w}_{k'} \mathbf{w}_{k'}^{\mathrm{H}} \mathbf{h}_k + \sum\limits_{k' \in \mathcal{K}_{\mathrm{ul}}} p_{k'}^{\mathrm{ul}} |h_{k,k'}|^2 + \sigma_{\mathrm{dl}}^2, \quad k \in \mathcal{K}_{\mathrm{dl}} \end{cases} \tag{18}$$

$$\Gamma_{e_k}^{\mathrm{L},1} \triangleq \begin{cases} \sum\limits_{k' \in \mathcal{K}_{\mathrm{ul}}} p_{k'}^{\mathrm{ul}} |h_{e_k,k'}|^2 + \sum\limits_{k' \in \mathcal{K}_{\mathrm{dl}}} \mathbf{h}_{e_k}^{\mathrm{H}} \mathbf{w}_{k'} \mathbf{w}_{k'}^{\mathrm{H}} \mathbf{h}_{e_k} + \sigma_{\mathrm{dl}}^2, \quad k \in \mathcal{K}_{\mathrm{ul}} \\ \sum\limits_{k' \in \mathcal{K}_{\mathrm{dl}}} \mathbf{h}_{e_k}^{\mathrm{H}} \mathbf{w}_{k'} \mathbf{w}_{k'}^{\mathrm{H}} \mathbf{h}_{e_k} + \sum\limits_{k' \in \mathcal{K}_{\mathrm{ul}}} p_{k'}^{\mathrm{ul}} |h_{e_k,k'}|^2 + \sigma_{\mathrm{dl}}^2, \quad k \in \mathcal{K}_{\mathrm{dl}} \end{cases} \tag{21}$$

In order to mitigate such misalignment, we enforce a discrete solution by introducing a negative entropy penalty function [17]

$$\mathbb{P}(d_{mk}) \triangleq d_{mk} \log(d_{mk}) + (1 - d_{mk}) \log(1 - d_{mk}). \tag{22}$$

In addition, notice that the constraints (14f) and (14g) involve products of optimization variables $\mathbf{d}_k, \mathbf{w}_k, \mathbf{v}_k$, which can be decoupled by reformulating those constraints as

$$\left\| \begin{matrix} 2w_{mk} \\ P_{\max} - d_{mk} \end{matrix} \right\|_2 \leq P_{\max} + d_{mk}, \ \forall k \in \mathcal{K}_{\mathrm{dl}}, \forall m \in \mathcal{M}. \tag{23}$$

$$\left\| \begin{matrix} 2v_{mk} \\ 1 - d_{mk} \end{matrix} \right\|_2 \leq 1 + d_{mk}, \ \forall k \in \mathcal{K}_{\mathrm{ul}}, \forall m \in \mathcal{M}, \tag{24}$$

All in all, the proposed design is given by the solution to the convex optimization problem.

$$\underset{\mathbf{D}_k, \mathbf{w}_k, \mathbf{v}_k}{\text{maximize}} \quad f^{\mathrm{o}}(\mathbf{w}_k, \mathbf{v}_k, \mathbf{D}_k) + \sum_{m \in \mathcal{M}} \sum_{k \in \mathcal{K}} \lambda d_{mk} \nabla \mathbb{P} \tag{25a}$$

$$\text{subject to} \quad 0 \leq d_{mk} \leq 1, \forall m \in \mathcal{M}, \forall k \in \mathcal{K}, \tag{25b}$$

$$(14c) - (14e), (23) - (24), \tag{25c}$$

where λ is a hyper-parameter updated progressively during the iterations of the procedure, and t_λ is a constant that determines the rate of such updates.

Algorithm 1 Secrecy Rate Maximization

Input Parameters: $t_{\max}$, t_λ and $\eta_{\mathrm{cf},k}$, $\forall k \in \mathcal{K}$.
Output: $\mathbf{D}_k \in \{0,1\}^{M \times M}, \mathbf{w}_k, \mathbf{v}_k \ \ \forall k \in \mathcal{K}$

Initialize
$\lambda \leftarrow 0$, $t \leftarrow 0$, $\mathbf{w}_k = \mathbf{h}_k, \ \forall k \in \mathcal{K}_{\mathrm{dl}}$, $\mathbf{v}_k = \mathbf{h}_k, \ \forall k \in \mathcal{K}_{\mathrm{ul}}$
Repeat
$\Omega_k^{\mathrm{I}} \leftarrow \log_2(1 + \eta_k^{\mathrm{I}}) - \eta_k^{\mathrm{I}}, \ \Omega_{e_k}^{\mathrm{L}} \leftarrow \log_2(1 + \tilde{\eta}_{e_k}^{\mathrm{L}})^{-1} - \tilde{\eta^{\mathrm{L}}}_{e_k}^{-1} \ \ \forall k \in \mathcal{K}$;
$\Upsilon_k^{\mathrm{I}} \leftarrow 2\sqrt{1 + \eta_k^{\mathrm{I}}}, \ \Upsilon_{e_k}^{\mathrm{L}} \leftarrow 2\sqrt{(1 + \tilde{\eta}_{e_k}^{\mathrm{L}})^{-1}} \ \ \forall k \in \mathcal{K}$;
Update $\Gamma_k^{\mathrm{I},1}, \ \Gamma_k^{\mathrm{I},2} \ \ \forall k \in \mathcal{K}$ as in equation (17), (18);
Update $\Gamma_k^{\mathrm{L},1}, \ \Gamma_k^{\mathrm{L},2} \ \ \forall k \in \mathcal{K}$ as in equation (21), (20);
$s_k^{\mathrm{I}} \leftarrow \Gamma_k^{\mathrm{I},1} \sqrt{1 + \eta_k^{\mathrm{I}}} / \Gamma_k^{\mathrm{I},2}, s_{e_k}^{\mathrm{L}} \leftarrow \Gamma_{e_k}^{\mathrm{L},1} \sqrt{(1 + \tilde{\eta}_{e_k}^{\mathrm{L}})^{-1}} / \Gamma_{e_k}^{\mathrm{L},2}$;
Update $\mathbf{D}_k, \mathbf{w}_k, \mathbf{v}_k, \ \forall k \in \mathcal{K}$ by solving optimization (25)
if $t \geq t_\lambda$ **then**
  $\lambda \leftarrow \lambda + 1$;
end if
Increment iteration counter $t \leftarrow t + 1$;
until convergence or $t = t_{\max}$

The pseudocode of the proposed method is summarized in Algorithm 1, and $(\cdot)^{t-1}$ denotes the solution obtained in the $t-1$ iteration. We emphasize that the initial beamformer can be obtained via the well-known maximum ratio combiner (MRC).

IV. Numerical results

In this section, we evaluate the SE and the secrecy capacity of the proposed method by computer simulations. The APs and UEs are assumed to be distributed at random and uniformly – *i.e.*, following a two-dimensional Poison point process (2D-PPP) [18] – within a communication area of 1×1 [km^2]. The large-scale fading term β is determined according to the urban model in [13]. The CVX [19] is used to solve equation (25). Other simulation parameters are summarized in Table I.

A. Benchmark System: TDD Cell-Free Massive MIMO

To evaluate the performance of the proposed method, we consider a comparison against a state-of-the-art (SotA) TDD-based CF-mMIMO, where downlink UEs in the communication area are potential eavesdroppers, as they would in the NAFD-CF-mMIMO. The SE in TDD CF-mMIMO can be expressed as [4] [5],

$$\zeta_k^{\mathrm{TDD}} \triangleq \begin{cases} R \cdot \log_2(1 + \eta_k^{\mathrm{TDD}}), & \forall k \in \mathcal{K}_{\mathrm{ul}}, \\ (1 - R) \cdot \log_2(1 + \eta_k^{\mathrm{TDD}}), & \forall k \in \mathcal{K}_{\mathrm{dl}}. \end{cases} \tag{26}$$

where $0 \leq R \leq 1$ denotes the ratio of uplink UEs in the service area.

The SINR for uplink and downlink transmissions are defined by the following equations, respectively.

$$\eta_k^{\mathrm{TDD}} \triangleq \begin{cases} \dfrac{p_k^{\mathrm{ul}} |\mathbf{v}_k^{\mathrm{H}} \mathbf{h}_k|^2}{\sum_{k' \in \mathcal{K}_{\mathrm{ul}} \setminus \{k\}} p_{k'}^{\mathrm{ul}} |\mathbf{v}_k^{\mathrm{H}} \mathbf{h}_{k'}|^2 + \sigma_{\mathrm{ul}}^2 \|\mathbf{v}_k^{\mathrm{H}}\|^2}, & \forall k \in \mathcal{K}_{\mathrm{ul}}, \\ \dfrac{|\mathbf{h}_k^{\mathrm{H}} \mathbf{w}_k|^2}{\sum_{k' \in \mathcal{K}_{\mathrm{dl}} \setminus \{k\}} |\mathbf{h}_k^{\mathrm{H}} \mathbf{w}_{k'}|^2 + \sigma_{\mathrm{dl}}^2}, & \forall k \in \mathcal{K}_{\mathrm{dl}}. \end{cases} \tag{27}$$

TABLE I
Simulation parameters

Parameter	Variable	Value
One side length of square service area	D	500 m
Maximum number of assigned APs	T	30
Maximum number of iterations	$t_{\max}$	30
Number of UEs	K	20
Ratio of uplink UEs	R	0.5
Carrier frequency	f_c	1.9 GHz
Bandwidth	B	20 MHz
Noise variance	$\sigma_{\mathrm{ul,dl}}^2$	-96 dBm
Maximum transmit power of each AP	$P_{\max}$	23 dBm
Transmit power of each UE	p_k^{ul}	20 dBm

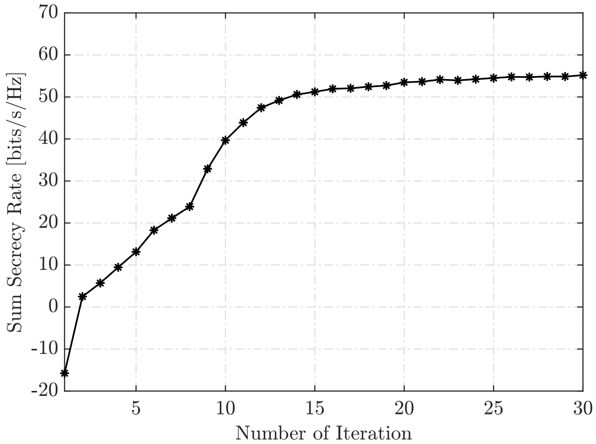

Fig. 1. Average aggregate secrecy achieved by Algorithm 1 as a function the number of iterations.

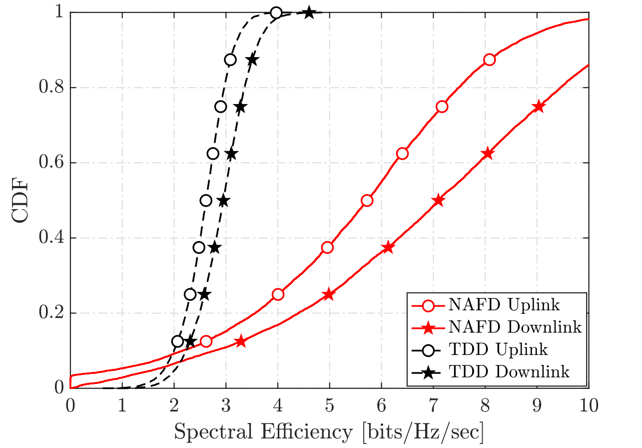

Fig. 2. Cumulative distribution function of per-user SE at uplink and downlink with proposed NAFD-based and SotA TDD-based CF-mMIMO systems.

As in the above, beamforming optimization is designed to maximize just for communication SE without considering the presence potential eavesdroppers as

$$\underset{\mathbf{w}_k,\mathbf{v}_k}{\text{maximize}} \left(\prod_{k\in\mathcal{K}} \zeta_k^{\text{TDD}} \right)^{\frac{1}{K}} \tag{28a}$$

$$\text{subject to} \sum_{k\in\mathcal{K}_{\text{dl}}} |w_{mk}|^2 \leq P_{\max}, \forall m \in \mathcal{M}, \tag{28b}$$

$$\sum_{k\in\mathcal{K}_{\text{ul}}} |v_{mk}|^2 \leq 1, \forall\ m \in \mathcal{M}. \tag{28c}$$

The objective function of problem (28) is also relaxed into a convex function via LDT and QT, and the solution is obtained by an iterative algorithm similar to Algorithm 1.

B. Convergence Evaluation

Let us start by evaluating the convergence of the proposed method summarized in Algorithm 1. To that end, Figure 1 shows the average aggregate secrecy rate achieved by the proposed scheme as a function of the number of iterations of Algorithm 1. The figure is obtained by averaging random deployment, channel and noise realizations, with the hyperparameter λ were updated at the $t_\lambda = 14$th iteration. The figure shows that the algorithm converges in average after approximately 20 iterations. Based on this result, in what follows, performances will be evaluated by setting the maximum number of iterations $t_{\max}$ to 20.

C. SE Performance Evaluation

Next, we evaluate the communication rates achieved be individual users at both downlink and uplink transmission, under both the proposed NADF-CFmMIMO scheme and the TDD-based SotA alternative. Figure 2, which shows a comparison of the cummutative distribution function (CDF) of such achieved rates, indicates that the proposed beamforming and clustering method can indeed realize full-duplex communication in the entire network with fair resource allocation for uplink and downlink, all while can achieve better SE over most realizations.

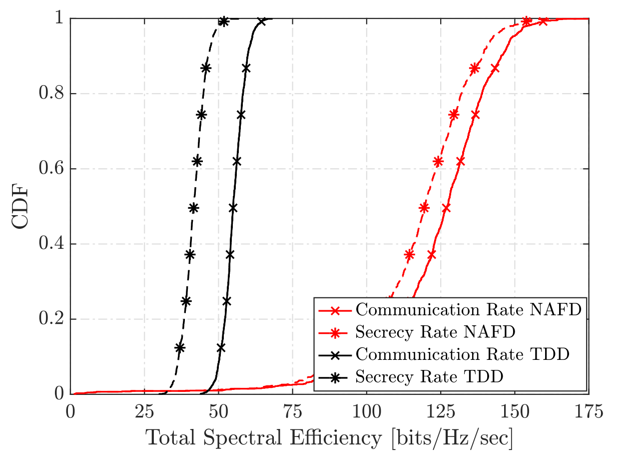

Fig. 3. Cumulative distribution function of aggregate communication and secrecy rates achieved at uplink and downlink with proposed NAFD-based and SotA TDD-based CF-mMIMO systems.

It is also observed that for about 10% of the UEs, however, the performance of NADF-CFmMIMO is slightly degraded compared to the SotA TDD scheme, both at uplink and downlink. This result may be explained by the fact that in some realizations in which UEs are closed located, NAFD CF-mMIMO, even with optimized beamforming and clustering, may still fail to suppress the mutual interference between uplink and downlink transmissions, especially because the single-antenna UEs do not have sufficient spatial degree of freedom. It can be expected that this result can be improved in a scenario where UEs have multiple antennas, but in any case, the relative degradation compared to the SotA TDD-based system is very small, such that we leave this line of work for others to possibly follow.

The latter statement is further motivated by the results shown in Figure 3, where the aggregate SE and secrecy rates of the proposed NAFD-CF-mMIMO and SotA TDD-based alternative are compared. The figure shows that the NAFD-CF-mMIMO system has a superior performance at least 90% of random realizations compared to the TDD system, and the achievable performances are approximately twice.

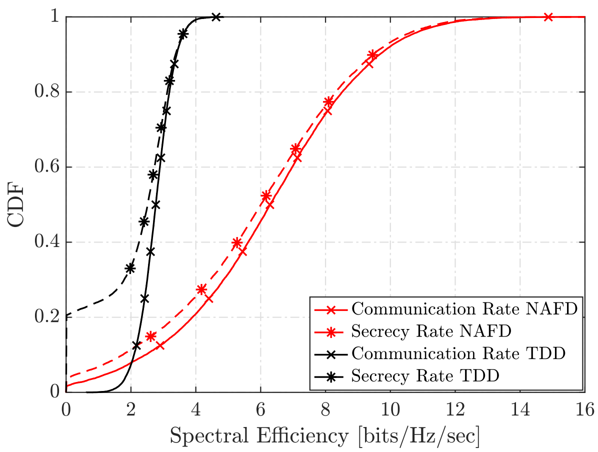

Fig. 4. Cumulative distribution functions of per-user communications and secrecy rates at uplink and downlink with proposed NAFD-based and SotA TDD-based CF-mMIMO systems.

The results confirm that the proposed NAFD system with the beamforming and AP clustering can generally achieve higher SE while guaranteeing very high secrecy capacity for the entire system compared to the conventional TDD system.

Finally, we evaluate in Figure 4 the per-user SE and the secrecy capacity of the proposed and SotA system each UE. The results show that the proposed NAFD-CF-mMIMO system exhibits superior SE compared to TDD alternative in more than 90% of random realizations, while in about 10% of the cases, a small degradation results from unmitigated mutual interference between uplink and downlink transmissions. In particular, it is found that the NAFD-CF-mMIMO system has zero UE capacity in about 5% of the regions, while the TDD system has zero UE capacity in more than 20% of the regions. Therefore, the NAFD scheme based on the proposed beamforming clustering design not only shows better overall system performance than the TDD SotA scheme, but also that it can achieve high transmission rates to a larger number of UEs while maintaining high confidentiality.

V. Conclusion

We proposed a joint design of AP clustering and beamforming based on the geometric mean maximization of the secrecy capacity in NAFD-CF-mMIMO systems, where the secret capacity of a given user is defined by regarding all other users in the coverage area as potential eavesdroppers. Numerical results demonstrated that the proposed method is able to achieve a higher secrecy capacity than the SotA TDD-based CF-mMIMO systems, while preserving a higher SE in most channel realizations.

Acknowledgement

This work was supported by JST, CRONOS, Japan Grant Number JPMJCS24N1.

References

[1] I. B. Djordjevic, "OAM-based hybrid free-space optical-terahertz multidimensional coded modulation and physical-layer security," *IEEE Photon. J.*, vol. 9, no. 4, pp. 1–12, Jul. 2017.

[2] A. Kalantari, M. Soltanalian, S. Maleki, S. Chatzinotas, and B. Ottersten, "Directional modulation via symbol-level precoding: A way to enhance security," *IEEE J. of Sel. Topics in Signal Process.*, vol. 10, no. 8, pp. 1478–1493, Aug. 2016.

[3] S. Leung-Yan-Cheong and M. Hellman, "The gaussian wire-tap channel," *IEEE Trans. on Inf. Theory*, vol. 24, no. 4, pp. 451–456, Jan. 1978.

[4] H. Q. Ngo, A. Ashikhmin, H. Yang, E. G. Larsson, and T. L. Marzetta, "Cell-free massive MIMO versus small cells," *IEEE Trans. Wireless Commun.*, vol. 16, no. 3, pp. 1834–1850, Mar. 2017.

[5] E. Björnson and L. Sanguinetti, "Scalable cell-free massive MIMO systems," *IEEE Trans. Commun.*, vol. 68, no. 7, pp. 4247–4261, Apr. 2020.

[6] ——, "Making cell-free massive MIMO competitive with MMSE processing and centralized implementation," *IEEE Trans. Wireless Commun.*, vol. 19, no. 1, pp. 77–90, Jan. 2019.

[7] I. A. M. Sandoval, K. Ando, O. Taghizadeh, and G. T. F. De Abreu, "Sum-rate maximization and leakage minimization for multi-user cell-free massive MIMO systems," *IEEE Access*, vol. 11, pp. 127 509–127 525, Nov. 2023.

[8] S. Fukue, H. Iimori, G. T. F. De Abreu, and K. Ishibashi, "Joint access configuration and beamforming for cell-free massive MIMO systems with dynamic TDD," *IEEE Access*, vol. 10, pp. 40 130–40 149, Apr. 2022.

[9] D. Wang, M. Wang, P. Zhu, J. Li, J. Wang, and X. You, "Performance of network-assisted full-duplex for cell-free massive MIMO," *IEEE Trans. Commun.*, vol. 68, no. 3, pp. 1464–1478, Dec. 2019.

[10] K. Okui, K. Ando, G. T. F. De Abreu, and K. Ishibashi, "Scalable network-assisted full-duplex cell-free massive MIMO with limited fronthaul capacity," in *Proc 2023 IEEE 98th Veh. Tech. Conf. (VTC2023-Fall)*, Oct. 2023, pp. 1–5.

[11] S. Fukue, G. T. F. De Abreu, and K. Ishibashi, "Network-assisted full-duplex millimeter-wave cell-free massive MIMO with localization-aided inter-user channel estimation," in *2023 Int. Conf. on Inf. Netw. (ICOIN)*, Jan. 2023, pp. 13–18.

[12] H. Iimori, J. Huschke, and J. Vieira, "Radio unit configuration for dynamic time division duplex in distributed MIMO systems," in *GLOBECOM 2023 - 2023 IEEE Global Commun. Conf.*, Feb. 2023, pp. 2542–2547.

[13] A. Tang, J. Sun, and K. Gong, "Mobile propagation loss with a low base station antenna for NLOS street microcells in urban area," in *Proc. IEEE VTS 53rd Veh. Technol. Conf., Spring 2001.*, vol. 1, Aug. 2001, pp. 333–336.

[14] K. Shen and W. Yu, "Fractional programming for communication systems—part I: Power control and beamforming," *IEEE Trans. Signal Process.*, vol. 66, no. 10, pp. 2616–2630, Mar. 2018.

[15] ——, "Fractional programming for communication systems—part II: Uplink scheduling via matching," *IEEE Trans. Signal Process.*, vol. 66, no. 10, pp. 2631–2644, Mar. 2018.

[16] Y.-F. Liu, T.-H. Chang, M. Hong, Z. Wu, A. M.-C. So, E. A. Jorswieck, and W. Yu, "A survey of recent advances in optimization methods for wireless communications," *IEEE J. on Sel. Areas in Commun.*, pp. 1–1, Aug. 2024.

[17] A. Bandi, B. S. Mysore R, S. Maleki, S. Chatzinotas, and B. Ottersten, "A novel approach to joint user selection and precoding for multiuser miso downlink channels," in *2018 IEEE Global Conf. on Sig. and Inf. Process. (GlobalSIP)*, Nov 2018, pp. 206–210.

[18] A. Baddeley, *Spatial Point Processes and their Applications*. Springer Berlin, 2007.

[19] M. Grant and S. Boyd, "CVX: Matlab software for disciplined convex programming, version 2.1," 2014.